

# Motion Planning for Cable-Suspended Payload Transportation with a Team of Multirotors in Cluttered Environments

Khaled Wahba and Wolfgang Hönig

**Abstract**—We propose a motion planner for cable-driven payload transportation using multiple unmanned aerial vehicles (UAVs) in an environment cluttered with obstacles. The planner considers both inter-robot and robot/obstacle collisions. The output of the planner is then tracked by our previously developed controller for payload transportation. We demonstrate the effectiveness of our approach through simulation experiments and an actual physical flight in a constrained environment with obstacles. The physical flight imitates a construction task where two multirotors carry a bridge in a cluttered environment and place it on two construction columns. We evaluate the performance for the proposed approach with respect to solution quality, computational effort, and success rate in different settings. Our experiments demonstrate the possibility of using multirotors for complex collaborative assistance in construction sites in the future.

## I. INTRODUCTION

Unmanned aerial vehicles (UAVs) are ideal for tasks that involve accessing remote locations, which makes them valuable collaborators in a variety of scenarios. Cable-driven payload transportation using multiple UAVs is well suited for collaborative assistance in construction sites such as carrying tools [1] or supporting bridge construction by transporting materials.

Control algorithms for payload transportation have advanced [2], [3], [4], [5], but inter-robot and robot/obstacle collisions are often not considered. Some methods address collision avoidance by using optimization techniques for the cable force allocation [6], [7], [8] or convexifying the cable constraints [9]. These either demand complex on-board computation or are limited by predefined cable regions. Other methods plan ahead with offline motion planners [10], [11] to address inter-robot and robot/obstacle collisions. The planners either use sampling-based approaches for the full system poses, or plan formations based on kinematic control. However, they do not reason over the load distribution over the multirotors. Thus, they might propose unfeasible configurations to be achieved by the planner.

We addressed the shortcomings of the mentioned methods through our previous work [12] by leveraging quadratic programs (QPs) and propose a QP-force allocation geometric controller that are executed on compute-constrained multirotors in realtime efficiently.

All authors are with Faculty of Electrical Engineering and Computer Science, Technical University of Berlin, Berlin, Germany {k.wahba, hoenig}@tu-berlin.de.

Video: [https://youtu.be/vKsa\\_Ali8OE](https://youtu.be/vKsa_Ali8OE)

The research was funded by the Deutsche Forschungsgemeinschaft (DFG, German Research Foundation) - 448549715.

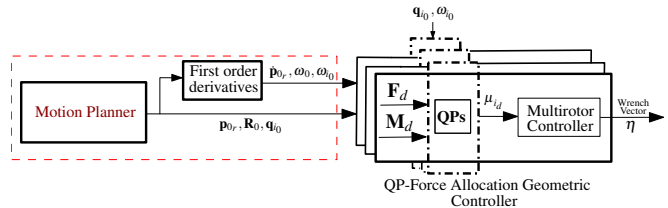


Fig. 1. Our contribution for this paper is highlighted in the red box. The output of the motion planner and its first order derivative define the full reference trajectory. The controller tracks the desired payload motions ( $\mathbf{F}_d, \mathbf{M}_d$ ) defined by the reference trajectory, and avoids inter-robot collisions, while taking into account the planned cable states ( $\mathbf{q}_{i0}, \boldsymbol{\omega}_{i0}$ ).

In this paper we extend our work [12] by proposing an offline motion planner for payload transportation in an environment cluttered with obstacles. We show our results on different simulation experiments and a physical flight on highly constrained embedded flight controllers in an environment with obstacles. The physical flight imitates a construction task where two quadrotors carry a bridge in a cluttered environment and place it on two construction columns.

## II. BACKGROUND

This section provides necessary background for the dynamic model and the used control design, see [12] for details.

### A. System Description

Consider a team of  $n$  quadrotors transporting a payload with massless cables. The payload is described as a rigid body with mass  $m_0$  and moment of inertia matrix  $\mathbf{J}_0$ . The cables are modeled as rigid rods each with length  $l_i$ . The state space vector is defined as

$$\mathbf{x} = (\mathbf{p}_0, \dot{\mathbf{p}}_0, \mathbf{R}_0, \boldsymbol{\omega}_0, \mathbf{q}_i, \boldsymbol{\omega}_i)^T \in \mathcal{C}, \quad i \in \{1, \dots, n\}, \quad (1)$$

where the configuration space  $\mathcal{C}$  is defined by: the pose of the payload  $\mathbf{p}_0 \in \mathbb{R}^3, \mathbf{R}_0 \in SO(3)$ ; the cable unit vector  $\mathbf{q}_i \in \mathbb{R}^3$  pointing to the quadrotor; and the payload and the cable angular velocities are  $\boldsymbol{\omega}_0 \in \mathbb{R}^3, \boldsymbol{\omega}_i \in \mathbb{R}^3$  respectively. The control input of the full system is defined as  $\mathbf{u} = (\boldsymbol{\eta}_1, \dots, \boldsymbol{\eta}_n)^T \in \mathcal{U} \subset \mathbb{R}^{4n}$ . Where  $\boldsymbol{\eta}_i = (f, \tau_x, \tau_y, \tau_z)^T$  is the thrust and torques controls of  $i$ -th quadrotor.

### B. Force Allocation Geometric Controller Overview

Our control design (see Fig. 1) extends the existing geometric controller [4] with an optimization-based cable force allocation method. Consider the desired control forces and moments that track the payload reference trajectory as  $\mathbf{F}_d, \mathbf{M}_d$  respectively. This method reformulates the cable forces allocation optimization problem as three consecutive

quadratic programs (QPs). The QPs solve for the desired cable forces  $\boldsymbol{\mu}_{i_d}$ , taking into account the inter-robot collisions, and track  $\mathbf{F}_d$  and  $\mathbf{M}_d$ . Thus,  $\boldsymbol{\mu}_{i_d}$  is tracked by the  $i$ -th UAV with a low-level controller [13].

**Desired Cable Forces** A significant advantage of the QPs formulation is that a user is able to specify a desired formation configuration based on another task objective (e.g. obstacle avoidance). Let us define  $\boldsymbol{\mu}_{i_0}$  as prespecified preferable cable forces such that  $\sum_i \boldsymbol{\mu}_{i_0} = \mathbf{F}_d$ . The cost function in the QPs can be modified as

$$c = \frac{1}{2} \|\boldsymbol{\mu}_{i_d}\|^2 + \lambda \|\boldsymbol{\mu}_{i_0} - \boldsymbol{\mu}_{i_d}\|^2, \quad (2)$$

where the first terms minimizes the sum of norms of the cable forces. The second term minimizes the difference between the cable forces and the preferred ones  $\boldsymbol{\mu}_{i_0}$  with  $\lambda$  as a weighting factor. Our previous work [12] proposed this method for a teleoperation task where the operator can switch to a predefined line formation to pass between two obstacles. Here, we use a motion planner to plan for both the desired payload poses and the preferred cable forces  $\boldsymbol{\mu}_{i_0}$ .

### III. APPROACH

#### A. Problem Statement

Consider the system described in Section II-A. The state space vector is defined by (1). The payload is transported in an environment defined by convex polytope workspace  $\mathcal{W} \subset \mathbb{R}^3$  with convex obstacles  $\mathcal{O}_1 \dots \mathcal{O}_{N_{\text{obs}}}$ . Let  $\mathbf{X} = \langle \mathbf{x}_0, \mathbf{x}_1, \dots, \mathbf{x}_T \rangle$  be a sequence of states sampled at time  $0, \Delta t, \dots, T\Delta t$  and  $\mathbf{U} = \langle \mathbf{u}_0, \mathbf{u}_1, \dots, \mathbf{u}_{T-1} \rangle$  be a sequence of controls applied to the system for times  $[0, \Delta t), [\Delta t, 2\Delta t), \dots, [(T-1)\Delta t, T\Delta t)$ , where  $\Delta t$  is a small timestep and the controls are constant during this timestep. Let us define a start state  $\mathbf{x}_s$  and a goal state  $\mathbf{x}_g$  in the collision-free configuration space  $\mathcal{C}_{\text{free}} \subset \mathcal{C}$ . Then our goal is to transport the payload from a start to a goal state in the minimal time  $T$ , which can be framed as the following optimization problem

$$\begin{aligned} \min_{\mathbf{X}, \mathbf{U}, T} \quad & J(\mathbf{X}, \mathbf{U}, T) \\ \text{s.t.} \quad & \begin{cases} \mathbf{x}_{k+1} = f(\mathbf{x}_k, \mathbf{u}_k) & \forall k \in \{0, \dots, T-1\} \\ \mathbf{u}_k \in \mathcal{U} & \forall k \in \{0, \dots, T-1\} \\ \mathbf{x}_0 = \mathbf{x}_s, \quad \mathbf{x}_T = \mathbf{x}_f \\ \mathbf{x}_k \in \mathcal{C}_{\text{free}} & \forall k \in \{0, \dots, T\} \\ \|\mathbf{p}_i - \mathbf{p}_j\| \geq r_i + r_j & \forall i \neq j, \end{cases} \end{aligned} \quad (3)$$

where the cost function  $J(\mathbf{X}, \mathbf{U}, T)$  can also minimize arbitrary task objectives (e.g., energy). The first equality constraint is the dynamic model of the system and the second constraint limits the control input within a feasible control space  $\mathcal{U}$  (e.g., actuator limits). The third set of constraints ensures that the motion connects the start and the goal states. The last two constraints ensure a collision-free path for the full state, where  $\mathbf{p}_i$  is the  $i$ -th quadrotor's position. The geometric shape of a robot is modeled as a sphere with radius  $r_i$  and the payload is modeled as a convex shape with  $\mathbf{p}_0 \in \mathbb{R}^3$  as the center of mass (CoM) position vector.

#### B. Overview

In order to solve the full optimization problem, we propose to divide it into sub-problems. We extend our previous work [12], with an offline geometric motion planner (see Fig. 1). The planner plans the payload and the cables geometric states jointly in the free space of the environment. The output of the planner is interpolated and used to compute the first order derivatives by numerical differentiation to define the reference trajectory. The reference trajectory is tracked by the QP-force allocation geometric controller. In particular, the planned cable states compute the desired cable forces  $\boldsymbol{\mu}_{i_0}$  by rescaling  $\mathbf{q}_{i_0}$  such that  $\sum_i \boldsymbol{\mu}_{i_0} = \mathbf{F}_d$  (see Section II-B). The augmentation of the motion planner with the controller ensures inter-robot and robot/obstacle collision avoidance. In terms of the motion planner, avoiding obstacles and inter-robot collisions are considered as a hard constraint. For the controller, it avoids inter-robot collision while tracking the payload reference trajectory simultaneously. However, it considers the robot/obstacle collision avoidance as a soft constraint by tracking  $\boldsymbol{\mu}_{i_0}$  as shown in (2).

#### C. Motion Planning

Given a start state  $\mathbf{x}_s$  and a goal state  $\mathbf{x}_g$  in an environment with convex obstacles  $\mathcal{O}_1 \dots \mathcal{O}_{N_{\text{obs}}}$ , we propose to use a sampling-based motion planner to plan a collision-free geometric path  $\mathbf{X}_{\text{geom}}$  for the following state vector

$$\mathbf{x}_{\text{geom}} = (\mathbf{p}_{0_r}, \mathbf{R}_{0_r}, \mathbf{q}_{1_0}, \dots, \mathbf{q}_{n_0})^T, \quad (4)$$

where  $\mathbf{x}_{\text{geom}} \in \mathbb{R}^3 \times SO(3) \times \mathbb{R}^{3n}$ . Consequently,  $\mathbf{X}_{\text{geom}}$  is interpolated and the first order derivatives are computed by numerical differentiation to define the full reference trajectory.

Consider the following relation between each desired cable force and its corresponding cable unit vector

$$\mathbf{q}_{i_0} = -\frac{\boldsymbol{\mu}_{i_0}}{\|\boldsymbol{\mu}_{i_0}\|}. \quad (5)$$

Thus,  $\boldsymbol{\mu}_{i_0}$  can be computed given the planned cable unit vectors that corresponds to a preferred formation. Consider distributing the magnitude of the desired motion  $\mathbf{F}_d$  of the payload per each cable as  $f_i = \frac{\|\mathbf{F}_d\|}{n}$ , where  $i \in \{1, \dots, n\}$  for  $n$  quadrotors. The resulting force  $\boldsymbol{\mu}_{i_0}$  for each cable is computed by rescaling the planned cable unit vectors as

$$\boldsymbol{\mu}_{i_0} = -f_i \mathbf{q}_{i_0}. \quad (6)$$

We use the following two extensions to to reduce the effect of the high dimensional state space of the payload transport system and to find high-quality solutions.

1) *State Space Representation*: We propose to reduce the state space size directly by using different representations for part of the state space. In particular, another representation for the unit vector  $\mathbf{q}_i \in \mathbb{R}^3$  is to use the azimuth  $\alpha_i$  and elevation  $\gamma_i$  angles, such that

$$\mathbf{q}_i = (\cos(\alpha_i) \cos(\gamma_i), \sin(\alpha_i) \cos(\gamma_i), \sin(\gamma_i))^T, \quad (7)$$

where  $\alpha_i \in [0, 2\pi)$  and  $\gamma_i \in [0, \pi/2)$ . Thus, the reduced state vector can be represented by

$$\mathbf{x}_r = (\mathbf{p}_{0_r}, \mathbf{R}_{0_r}, \alpha_1, \gamma_1, \dots, \alpha_n, \gamma_n)^T. \quad (8)$$

TABLE I

SIMULATION RESULTS. SHOWN ARE MEAN VALUES FOR THE COST AND TIME OF THE FIRST SOLUTION OVER 10 RUNS WITH A TIMELIMIT OF 750 sec FOR DIFFERENT SCENARIOS USING DIFFERENT NUMBER OF ROBOTS, EACH WITH STANDARD DEVIATION (SMALL GRAY).

Environment	Metrics	3 robots	4 robots	5 robots	6 robots	7 robots	8 robots
Empty	Cost	5.15 <small>0.72</small>	5.76 <small>0.21</small>	<b>4.29</b> <small>0.00</small>	4.49 <small>0.00</small>	4.75 <small>0.00</small>	4.75 <small>0.00</small>
	Time [sec]	0.05 <small>0.03</small>	0.05 <small>0.01</small>	0.04 <small>0.02</small>	<b>0.04</b> <small>0.01</small>	0.05 <small>0.00</small>	0.05 <small>0.01</small>
	Success Rate [%]	100	100	100	100	100	100
Forest	Cost	<b>10.86</b> <small>4.56</small>	19.22 <small>15.94</small>	30.26 <small>10.72</small>	15.49 <small>0.00</small>	-	-
	Time [sec]	<b>11.42</b> <small>10.75</small>	33.22 <small>32.93</small>	297.08 <small>114.17</small>	631.48 <small>4.58</small>	-	-
	Success Rate [%]	100	100	80	20	-	-
Maze	Cost	10.92 <small>5.85</small>	23.81 <small>18.86</small>	13.56 <small>5.24</small>	<b>9.65</b> <small>0.00</small>	-	-
	Time [sec]	<b>0.50</b> <small>0.42</small>	6.35 <small>6.86</small>	40.66 <small>37.91</small>	172.25 <small>0.00</small>	-	-
	Success Rate [%]	100	100	100	10	-	-

2) *Cost Function*: To converge to an optimal solution, a cost function is required. Given two consecutive states as  $\mathbf{x}_r(k)$  and  $\mathbf{x}_r(k+1)$ , we propose to use a cost function that minimizes the integral of the energy between the two states. First, let us define the  $\mathbf{q}_{i_{\text{base}}} = (0, 0, 1)^T$  as the desired cable direction to carry the payload statically. Consider the required force magnitude to carry a unit payload mass with respect to the static case (i.e., all cables point towards  $\mathbf{q}_{i_{\text{base}}}$ ) as

$$F(k) = \frac{1}{n} \sum_{i=1}^n \frac{1}{\mathbf{q}_{i_{\text{base}}} \cdot \mathbf{q}_i(k)}, \quad (9)$$

where  $(\cdot)$  is the dot product and  $n$  is the number of cables. We assume a trapezoidal energy profile between two consecutive states. Thus, the cost function is

$$c = \frac{F(k) + F(k+1)}{2} \|\mathbf{p}_0(k) - \mathbf{p}_0(k+1)\|, \quad (10)$$

where  $\|\mathbf{p}_0(k) - \mathbf{p}_0(k+1)\|$  is the Euclidean distance of the payload position. The sampler will converge to the minimum cost solution over time. The accepted samples by the collision checker will ensure that the current formation configuration distributes the load over the cables compared to the static case.

After generating the plan and computing the derivatives for the payload pose and the cable directions, the reference trajectories are provided to the QP-force allocation geometric controller. In particular, the payload pose and velocity reference trajectories are used to compute  $\mathbf{F}_d$  and  $\mathbf{M}_d$ , while the planned  $(\alpha_i, \gamma_i)$  for each cable are used to compute the cable directions  $\mathbf{q}_{i_0}$  using (7). Finally, the preferred desired cable forces  $\boldsymbol{\mu}_{i_0}$  are computed with (6) for each cable, which is tracked the QPs based on the cost function (2).

#### IV. EXPERIMENTAL RESULTS

To validate the performance of our method, we provide three simulation experiments and a physical flight. In particular, we implemented the sampling-based motion planner using OMPL [14], a widely used C++ library, and meshcat to visualize the output.

The simulation environments are bounded, where the bounds only limit the translational part of the payload, i.e., the cables and the robots are allowed to be outside.

We use RRT\* as the sampling motion planner for all our experiments. All environments use simple geometric

sphere, cylinder, and box shapes to model the quadrotors, the obstacles, the payload, and the cables for efficient collision checking. Collision checking is done using FCL (Flexible Collision Library) in all cases.

All scenarios for the motion planning experiments were solved on a workstation (AMD Ryzen Threadripper PRO 5975WX @ 3.6 GHz, 64 GB RAM, Ubuntu 22.04).

#### A. Simulations

For the simulations, we consider a triangular rigid payload ( $8 \times 8 \times 1$  cm) carried by multiple (up to 8) quadrotors with cables. We test our motion planning approach on three different scenarios, see Table I and the supplemental video: obstacle-free (i.e., Empty), a random forest-like environment, and a maze-like environment, where the payload is transported through a narrow passage of two cylindrical obstacles.

*Performance Evaluation*: We summarize the main results as follows. The motion planner finds first solutions with high success rates and relatively low costs quickly for obstacle-free scenarios.

In cluttered environments (forest and maze) the success rate decreases as the number of robots increase. Two examples show the convergence behavior of the solution quality (cost) in Fig. 2. However, our approach fails to find solutions for seven and eight robots, only. This is due to the curse-of-dimensionality and our choice of using rejection sampling in OMPL. With rejection sampling, the probability of sampling pairwise collision-free cable angles quickly becomes zero as the number of robots increase, if the payload is very small in size as in our simulations. Sampling valid states directly can mitigate the effect and is an interesting avenue for future work.

Currently we define the full goal state configuration, and we believe this provides unfair hints for the planner, as there might be other goal states with lower costs. Moreover, specifying the full goal configuration requires domain knowledge to set up the problem, which becomes complex with more robots. Instead, defining goal regions for the cable angles will provide better solutions quality.

#### B. Physical Flights

We are interested in imitating a construction task, see the supplemental video. Two quadrotors are required to initially take off from the ground and carry a bridge (i.e., a rod).

## V. CONCLUSION

In this paper we present a geometric motion planner for the cable-suspended payload transport using multiple UAVs in an environment with obstacles. We rely on sampling-based approaches to generate a plan for the geometric states of the system while avoiding obstacles and inter-robot collisions. The plan is then tracked by the QP-force allocation geometric controller from our previous work.

We demonstrate the feasibility and effectiveness of our approach with three simulation experiments and an actual physical flight. The physical flight imitates a construction task where two quadrotors carry a bridge in a cluttered environment and place it on two construction columns.

Our results indicate the potential of using our approach for more complex construction tasks with enhancements in scalability and solution quality. In the future, we are aiming to extend our planner to more realistic construction scenarios, including cases where multiple robot teams operate in the same shared environment.

## REFERENCES

- [1] C. Gabellieri, M. Tognon, L. Pallottino, and A. Franchi, "A study on force-based collaboration in flying swarms," in *Int. Conf. Swarm Intell.*, 2018, pp. 3–15.
- [2] A. Tagliabue, M. Kamel, R. Siegwart, and J. Nieto, "Robust collaborative object transportation using multiple mavs," *I. J. Robotics Res.*, vol. 38, no. 9, pp. 1020–1044, 2019.
- [3] M. Tognon, C. Gabellieri, L. Pallottino, and A. Franchi, "Aerial co-manipulation with cables: The role of internal force for equilibria, stability, and passivity," *IEEE Trans. Robot. Autom. Lett.*, vol. 3, no. 3, pp. 2577–2583, 2018.
- [4] T. Lee, "Geometric control of quadrotor uavs transporting a cable-suspended rigid body," *IEEE Trans. on Control Syst. Tech.*, vol. 26, no. 1, pp. 255–264, 2017.
- [5] D. Six, S. Briot, A. Chriette, and P. Martinet, "The kinematics, dynamics and control of a flying parallel robot with three quadrotors," *IEEE Trans. Robot. Autom. Lett.*, vol. 3, no. 1, pp. 559–566, 2017.
- [6] X. Liu, G. Li, and G. Loianno, "Safety-aware human-robot collaborative transportation and manipulation with multiple mavs," *arXiv preprint arXiv:2210.05894*, 2022.
- [7] S. Sun and A. Franchi, "Nonlinear mpc for full-pose manipulation of a cable-suspended load using multiple uavs," *arXiv preprint arXiv:2301.08545*, 2023.
- [8] Z. Li, J. F. Horn, and J. W. Langelaan, "Coordinated transport of a slung load by a team of autonomous rotorcraft," in *AIAA Guidance, Navigation, and Control Conference*, 2014, p. 0968.
- [9] J. Geng and J. W. Langelaan, "Cooperative transport of a slung load using load-leading control," *J. Guid., Control, Dyn.*, vol. 43, no. 7, pp. 1313–1331, 2020.
- [10] M. Manubens, D. Devaurs, L. Ros, and J. Cortés, "Motion planning for 6-d manipulation with aerial towed-cable systems," in *Robotics: science and systems (RSS)*, 2013, p. 8p.
- [11] H. G. De Marina and E. Smeur, "Flexible collaborative transportation by a team of rotorcraft," in *Proc. IEEE Int. Conf. Robot. Autom.* IEEE, 2019, pp. 1074–1080.
- [12] K. Wahba and W. Hönig, "Efficient optimization-based cable force allocation for geometric control of multiple quadrotors transporting a payload," *arXiv preprint arXiv:2304.02359*, 2023.
- [13] T. Lee, K. Sreenath, and V. Kumar, "Geometric control of cooperating multiple quadrotor uavs with a suspended payload," in *Proc. IEEE Conf. Decis. Control*, 2013, pp. 5510–5515.
- [14] I. A. Sucas, M. Moll, and L. E. Kavraki, "The open motion planning library," *IEEE Robotics & Automation Magazine*, vol. 19, no. 4, pp. 72–82, 2012.
- [15] J. Förster, "System identification of the crazyflie 2.0 nano quadcopter," B.S. thesis, ETH Zurich, 2015.

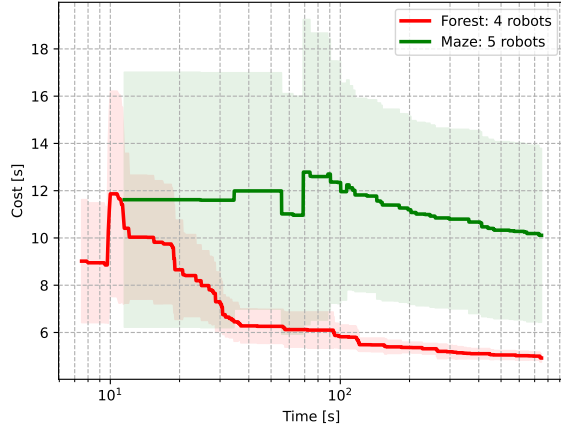


Fig. 2. Examples for the forest and maze environment with four and five robots, respectively. The plot shows the mean and standard deviation (shaded) for cost convergence over runtime (log-scale), if the success rate is over 50%.

Then, they carry the rod through a narrow passage between two obstacles and place it on top of two construction columns (i.e., the blue boxes) and finally, they land.

We generate an offline motion plan for two quadrotors carrying a rod payload through obstacles. Then, we provide the plan to be executed by the optimization-based force allocation geometric controller. To demonstrate the benefits of planning with the cable states, we compare two different executions: one that only tracks the given reference of the payload pose and one that includes the full geometric reference state including the planned cable states.

1) *Setup*: We use an 8 g rigid rod payload for our experiments. Moreover, We use quadrotors of type Bitcraze Crazyflie 2.1 (CF). These are small (9 cm rotor-to-rotor) and lightweight (34 g) products that are commercially available. The physical parameters are identified in prior work [15]. We rely on our prior software infrastructure [12], which includes the control algorithm in *C* to run directly on-board the STM32-based flight controller (168 MHz, 192 kB RAM), and Crazyswarm2 to communicate with the robots on the host side. The positions of both quadrotors and the pose of the payload are estimated using a motion capture system and streamed (along with the setpoints from the motion plan) to both quadrotors via broadcast communication at 100 Hz.

2) *Experimental Results*: When we provide the planned cable states to the controller, the payload tracking errors are 12.4 cm and 11.3°. However, if we provide the planned payload pose only, the tracking errors increase to 14.5 cm and 15.9°. Thus, using the full geometric reference state and in particular the planned cable states provide more accuracy for tracking the trajectory while avoiding the obstacles. This effect is also visually apparent during the takeoff sequence, which becomes smoother with the planned cable states.